ISSN 0742-0463, Journal of Volcanology and Seismology, 2007, Vol. 1, No. 5, pp. 333–348. © Pleiades Publishing, Ltd., 2007.
Original Russian Text © Yu.F. Kopnichev, I.N. Sokolova, 2007, published in Vulkanologiya i Seismologiya, 2007, No. 5, pp. 54–70.

Heterogeneities in the Field of Short Period Seismic Wave Attenuation in the Lithosphere of Central Tien Shan

Yu. F. Kopnichev[a] and I. N. Sokolova[b]

[a] *United Institute of Physics of the Earth, Russian Academy of Sciences, Moscow, 123995 Russia*
[b] *Institute of Geophysical Research, Nuclear Science Center, Kurchatov*

Received June 4, 2003

Abstract—Records of deep-focus Hindu Kush earthquakes in the depth ranges 70–110 and 190–230 km made by 45 digital and analogue seismic stations were analyzed to study the attenuation field of short period seismic waves in the lithosphere of central Tien Shan. The dynamic characteristics studied include the ratio of peak amplitudes in *S* and *P* waves (*S*/*P*) and the ratio of the *S*-wave maximum to the coda level in the range $t = 400 \pm 5$ s, where t is the lapse time (*S*/c400) for 1.25 Hz. Comparatively high values of *S*/*P* are shown to prevail in most of the area, corresponding to lower *S*-wave attenuation. Upon this background is a band of high and intermediate attenuation in the west of the area extending along the Talas–Fergana fault in the south and afterwards turning north-northeast. The rupture areas of the two largest ($M \geq 7.0$) earthquakes which have occurred in Tien Shan during the last 25 years are confined to this band. Abnormally high values of *S*/c400 were obtained for stations situated in the rupture zone of the August 19, 1992, magnitude 7.3 Suusamyr earthquake and around it. For two of the stations we found considerable time variations in the coda envelope before the earthquake. The effective *Q* was derived from compressional and shear wave data for the entire area, as well as for the band of high attenuation. Comparison with previous data shows that the attenuation field in the area has changed appreciably during 20–25 years, which can only be due to a rearrangement of the fluid field in the crust and uppermost mantle. It is hypothesized that a large earthquake is very likely to occur in the northern part of the attenuating band.

DOI: 10.1134/S0742046307050065

INTRODUCTION

The short-period seismic-wave attenuation field in the crust and upper mantle supplies important information on earth properties in the lithosphere and asthenosphere. This primarily applies to shear waves whose response to the presence of a liquid phase, i.e., fluids or partially molten material, is the greatest. It is a well-known fact that a mere 1 per cent of liquid phase produces a 10% reduction in shear wave velocity and a dramatic increase in attenuation [27].

We note that heterogeneities in the shear wave velocity field are poorly known in the area. This is largely due to low arrival-time accuracy for short-period shear waves upon the background of a *P* coda at near and regional distances. The degree of heterogeneity in the shear wave velocity field for the Tien Shan crust can be inferred from results derived in [4] by applying the receiver function method to records of teleseismic earthquakes: the shear wave velocity in the upper crustal layer a few kilometers thick consisting of Paleozoic and Precambrian rocks may drop by about 30% compared with the normal value (this is thought to be due to considerable amounts of free fluids). That the shear wave velocity field in the area is poorly known is shown by the fact that the authors of [4] assumed no lateral velocity variations when determining the depth to the Moho from arrival times of converted waves.

The present study is concerned with the lateral variations in the attenuation field of shear and compressional waves in central Tien Shan. The data consist of unique experimental materials, the records of deep-focus Hindu Kush earthquakes made by 45 digital and analog seismic stations.

THE GEOLOGICAL AND GEOPHYSICAL BACKGROUND FOR THE AREA OF STUDY

The area of study is confined within 39°–45° N and 73°–81° E and contains much of central Tien Shan and adjacent regions—the southern margin of the Kazakh Platform which bounds it on the north and the northwesternmost part of the Tarim massif in the south (Fig. 1). The geosynclinal period in the evolution of most of Tien Shan terminated at the end of the Hercynian, the resulting platform experienced insignificant differentiated movements during Mesozoic time. Tectonic movements resumed since the end of the Paleogene, producing the Tien Shan mountain structures which are as high as 7.5 km [21].

Deep–seated fault zones have been very important during the whole of the tectonic evolution of Tien Shan. The faults cut through the entire crust, penetrate into the upper mantle, and are natural boundaries to major structural features. Most of the faults are high–angle

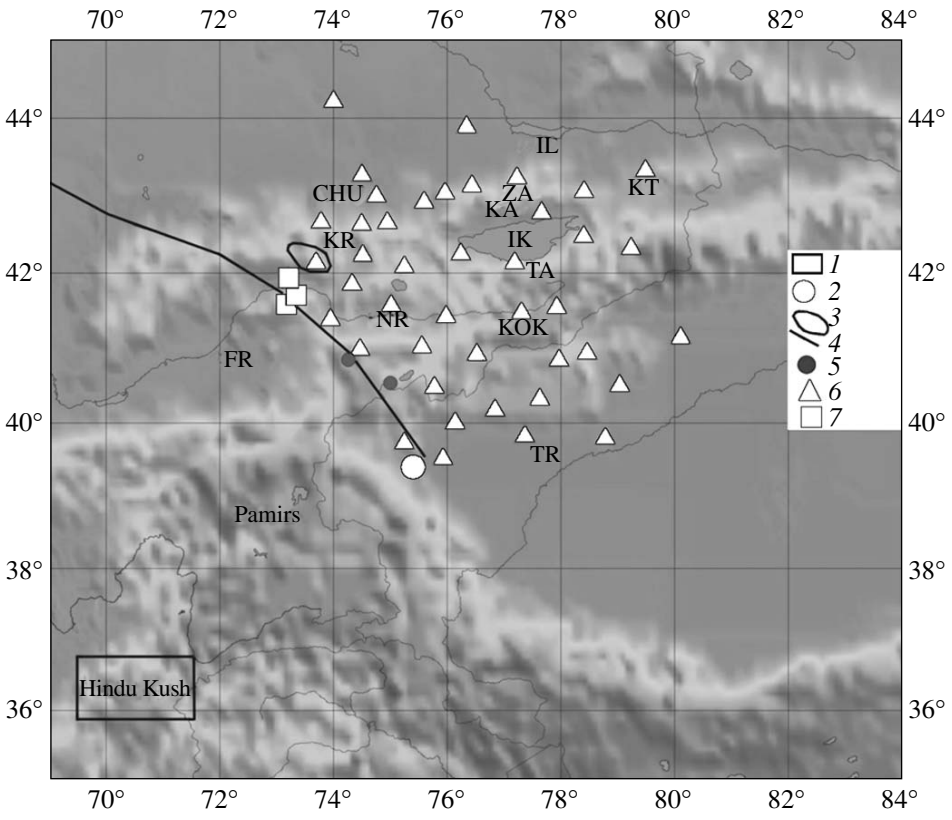

Fig. 1. Map of study area. (*1*) the source zone of Hindu Kush earthquakes, (*2*) epicenter of the August 23, 1985 Kashgar earthquake, (*3*) the rupture zone of the August 19, 1992 Susamyr earthquake, (*4*) Talas–Fergana fault, (*5*) springs with abnormally high helium isotope ratios, (*6*, *7*) seismic stations: (*6*) 1998–2000 data, (*7*) 1976–1992 data. Shown are mountain massifs and basins in central Tien Shan. Ranges: KR Kirgiz, ZA Zaili Alatau, KA Kungei Alatau, TA Terskei Alatau, KT Ketmen', KOK Kokshaal Tau. Basins: CHU Chuya, IL Ili, NR Naryn, FR Fergana, TR Tarim massif, IK Lake Issyk Kul'.

reverse, dipping at 70° or steeper [21]. Many fault zones exhibit high shear wave attenuation in the lower crust and uppermost mantle [11, 14, 20].

The crust in the Chu and Ili basins is 40–45 km thick, increasing to 55–60 km in the mountain areas of Tien Shan [31].

According to tomographic analyses, the upper mantle beneath Tien Shan has lower compressional velocities [33].

As to the level of seismicity, the area of study is one of the most active in the world. It is enough to state that three M > 8.0 earthquakes have occurred there during the past 115 years. Most of the larger (M > 6.0) earthquakes tend to occur on major fault zones.

THE DATA

Most of the seismic stations used were installed on Paleozoic outcrops. The stations in the margin of the Tarim massif and the ARA station stand on young Cenozoic or Quaternary rocks.

Most stations (38) are equipped with REFTEK three-component digital instruments. The records were made by STS-1, STS-2, CMG-3, CMG-40T, and L4C seismometers. We also used records of seven SKM-3 analog stations writing on photographic paper (KUU, TORK, NICH, KRSU, KST, MTB, and SATY).

We used seismograms of Hindu Kush earthquakes which are convenient in that representative experimental materials can be acquired during a comparatively short time. In all, there were about 800 records of earthquakes in the depth ranges h_0 = 70–110 and 190–230 km, at epicentral distances of 500 to 1100 km.

The 1998–2000 data were examined for most stations. For some stations which were situated near the rupture zone of the August 19, 1992 Suusamyr earthquake (Fig. 1) with magnitude M = 7.3 (TORK, NICH, and KRSU), we used analog data recorded in 1976–1992.

THE DATA PROCESSING TECHNIQUE

Our analysis of digital records involved narrowband frequency filtering of vertical components using filters centered at 0.6, 1.25, 2.5, and 5 Hz with 2/3-octave width at 0.7 of the maximum, similarly to those of the "frequency-selective station" [5]. We focused attention on the data in the most representative band of

1.25 Hz. Analog seismograms were first scanned by a large format scanner and digitized at a sampling rate of 20 Hz.

Figure 2 presents sample envelopes for a Hindu Kush earthquake in the 1.25 Hz band as recorded at several stations. It is apparent from this figure that the ratio of *S* to *P* amplitudes generally decreases with increasing epicentral distance. One notes that the *S* and *P* waves are very impulsive and the *S* coda amplitude rapidly decays at AML. This sort of record is also typical of EKS2, AAK, UCH, and TORK, all of these being installed close to the Susamyr earthquake rupture zone. The station TKM2, as well as TLG and KAR, have a very low level of *S* waves relative to *P* compared with near stations. At PIQG and most other stations in the northwestern margin of the Tarim, as well as at ARA, which are on young sedimentary rocks, the records frequently contain "diffuse" *P* and *S* groups involving a slow amplitude increase until the *S* onsets.

The attenuation field was examined here using the following parameters:

(1) The common logarithm of peak amplitude ratio in *S* and *P* at a frequency of 1.25 Hz (*S*/*P*). The peak amplitudes in compressional waves were measured in the 10-s interval from the onset and in shear waves in the interval ±10 s from the onset of *S* as predicted by the travel-time table.

(2) The common logarithm of *S*-wave maximum to the maximum coda level in the interval $t = 400 \pm 5$ s, where *t* is the lapse time (*S*/c400). In the range of epicentral distance used in this study, regular *S* and *P* waves from Hindu Kush earthquakes are incident at the M interface at low angles. Because the velocity heterogeneities in the lithosphere of the study area are not well enough known for analysis of wave paths with this dense station network (especially for shear waves), we have assumed a simple two-layer earth model for the sake of definiteness involving a 50-km crust with average shear velocities in the crust and upper mantle equal to 3.5 and 4.6 km/s, respectively [33]. (This model was used as a first approximation only because it is impossible to study velocity heterogeneities and attenuation at the same time.) In that case, for earthquakes at 100 and 200 km depth, the rays are incident on the M interface at angles of 83.5°–87° and 72°–81° with the vertical, respectively, while in the crust the values are 49.1°–49.5° and 46.4°–48.1° (in the distance range 550 to 1100 km) (Fig. 3).

From Figs. 3 and 4 it follows that the ray paths for near stations are sufficiently divergent in the crust and uppermost mantle only. At the same time, as will be shown below, the values of *S*/*P* may be very different, even for the nearest stations. We are going to estimate the divergence of rays for near stations at the same azimuth looking from the source (Fig. 4). The crustal thickness was assumed to be $h_M = 50$ km. Two cases are considered, $h_0 = 100$ and 200 km. It can be seen from Fig. 1 that the average interstation distance for near stations can be set equal to about $l \sim 70$ km. We now estimate the ray divergence for near stations at the same azimuth looking from the source. The angle with the vertical for the ray O_2BA toward the near station A is

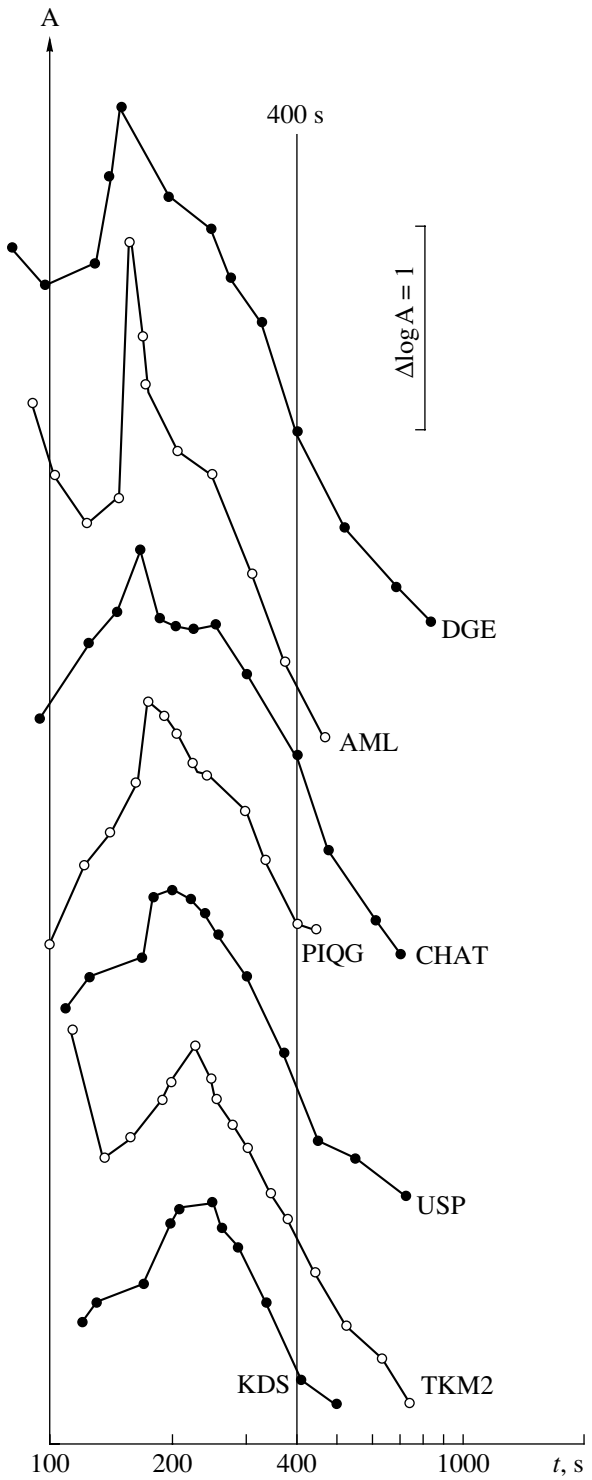

Fig. 2. Envelopes of records at several stations for the October 10, 1999 Hindu Kush earthquake (36.45° N, 70.64° E, *h* = 195 km). Vertical component, the 1.25 Hz channel.

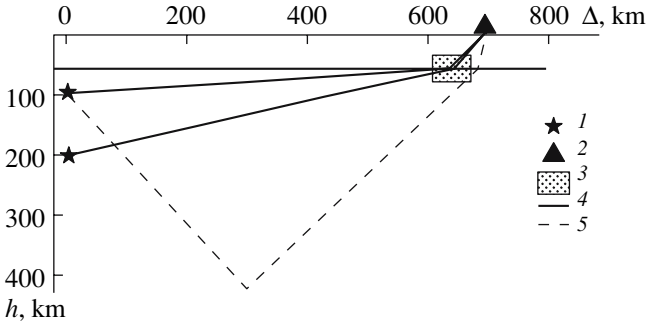

Fig. 3. Propagation of direct *S* and *P* waves, as well as the coda–forming *S* waves. (*1*) earthquake hypocenters, (*2*) seismic station, (*3*) zone of high attenuation in the lower crust and uppermost mantle, (*4*) rays of direct *S* and *P* waves, (*5*) the code-forming *S* waves.

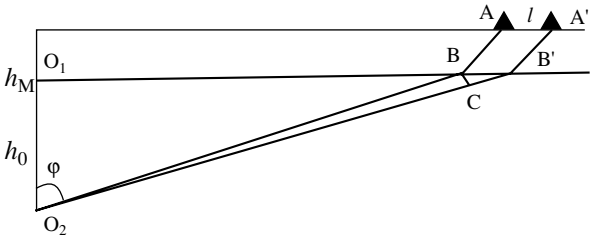

Fig. 4. Diagram illustrating ray divergence for near stations.

equal to $\varphi = \arctan(r/(h_0 - h_M)$, $r = O_1B$, while that for a more distant station it is A'—$\varphi' = \arctan(r'/(h_0 - h_M))$, ($r' = O_1B'$). The displacement of the ray $O_2B'A'$ relative to the ray O_2BA, which intersects the M interface at the point B (the segment BC), is equal to $d = r\sin(\varphi' - \varphi)/\sin\varphi$. Simple calculations will show that, when the epicentral distance Δ varies from 550 to 1100 km for hypocentral depths 100 and 200 km, the quantity *d* decreases from 6 to 4 km and from 18 to 10 km, respectively. It thus appears that the ray divergence in the region where ray 1 is incident on the M interface does not exceed 18 km. On the other hand, the Fresnel zone for the ray segment CB'A', which controls the signal amplitude at the point A', is equal to $R_f = \sqrt{L\lambda} \sim 30$ km for *P* and ~23 km for *S* waves (*L* is the segment length and λ the wavelength). Thus, in the overwhelming majority of cases the ray divergence at B and C for near stations is much (generally a few times) smaller than the Fresnel zone. From this it follows that all differences in the attenuation of *P* and *S* waves for the two stations considered are largely due to the crust (for station A), as well as to the uppermost mantle (at distances of about 50–130 km to the southwest) and to the crust (for station A'). Below we will discuss whether it is possible to get more accurate estimates of regions of high attenuation.

Kopnichev and colleagues [8, 10, 23] have shown that the coda of Hindu Kush earthquakes at frequencies about 1 Hz is mostly composed of shear waves reflected at numerous subhorizontal discontinuities in the crust and upper mantle. Figure 5 shows examples of coda polarization on AML records in the intervals $t = 200 \pm 5$, 300 ± 5, and 400 ± 5 s (for the 1.25 Hz filter). It can be seen in this Figure that the coda is mostly polarized in the horizontal plane (SH type), which is consistent with the conclusions reached in [8, 10, 23].

This model of coda generation involves *S* waves that traverse the lithosphere and asthenosphere at increasingly higher angles as time goes on. Consequently, the parameter *S*/c400 characterizes the change in *S*-wave attenuation as the station is approached (singly reflected *S* waves that arrive in the coda at $t \sim 400$ s are transmitted across the M interface at distances of about 10–15 km from the station).

It should be noted that high values of *S*/*P* and *S*/c400, as well as the impulsive character of regular waves at 1 Hz, can in principle, in some cases, have been caused by focusing of *S* and *P* waves. To test this possibility we considered spectral characteristics of records of some stations, including AML, for which very high values of *S*/c400 were obtained (Fig. 2). Figure 6 presents records of the October 10, 1999 earthquake ($h_0 = 195$ km) obtained by narrow-band filtering on channels centered at 0.6, 1.25, 2.5, and 5 Hz. One can see that the records of *P*, and especially of *S*, at AML have the highest frequencies, while those at TKM2 have the lowest frequency. Consequently, comparatively low attenuation of *S* waves is responsible for the high values of *S*/*P* and *S*/c400 rather than the focusing factor. As to the focusing of compressional waves, we note that there are practically no impulsive *P* waves on the 1.25 Hz channel in the records considered (Fig. 6). Lastly, simple estimates show that the focusing due to the Moho topography requires that the radius of curvature in the focusing elements (~5 km) must be several times smaller than the Fresnel zone, hence that effect cannot be significant in influencing the amplitudes of regular waves.

ANALYSIS OF THE DATA

Hypocenter depths 70–110 km. Figure 7 shows average *S*/*P* in relation to average epicentral distance for the depth range considered. It is seen that the parameter *S*/*P* for similar values of Δ can change by an order of magnitude (for the stations KOPG and TKM2). The standard deviations of the average *S*/*P* for different stations vary between 0.14 and 0.40.

The whole range of *S*/*P* was divided into three levels corresponding to lower, intermediate, and higher attenuation. We assumed (similarly to the range 190–230 km) that the intermediate attenuation corresponds to the values of *S*/*P* falling in the interval ±0.1 relative to the least squares regression line (Figs. 7, 8).

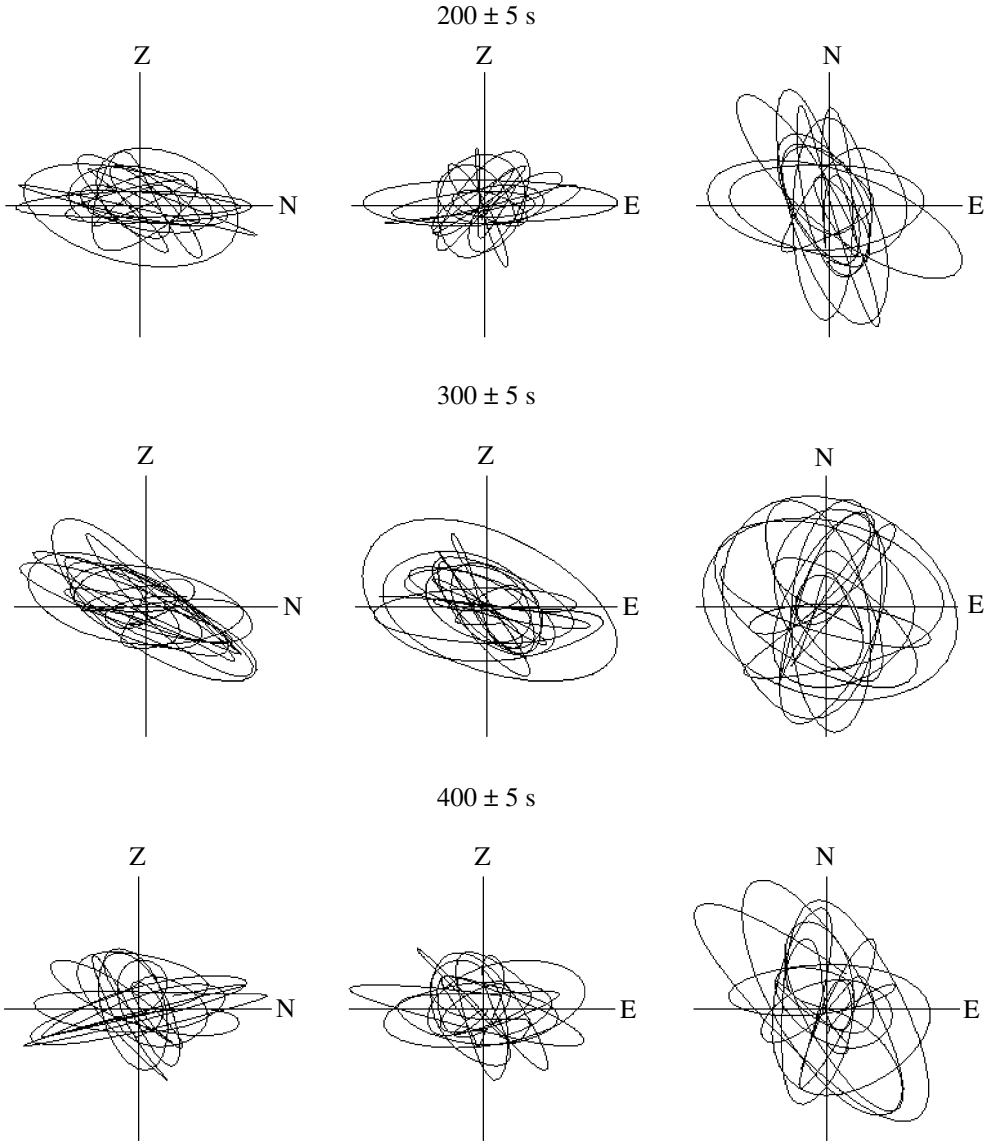

Fig. 5. Examples of coda polarization in the record of the October 10, 1999 earthquake at the station AML. The 1.25 Hz channel.

Lower and intermediate attenuation is generally observed for the margin of the Tarim massif, except for two western stations (KASH and TGMT). Comparatively low attenuation was also recorded at most stations situated in the north margins of major basins under which direct *P* and *S* are transmitted across the lower crust and uppermost mantle: USP (the Chu basin), ANA (the Issyk–Kul' basin), NRN (the Naryn basin), and KRSU (the Fergana basin). One exception is the station KAI for which *S*/*P* was about 0.4 below that for the near station NRN. Intermediate values of *S*/*P* were obtained for KHA (the southern margin of the Kazakh Platform).

It follows from Fig. 8 that comparatively high values of *S*/*P* prevail in most of the study area. Upon this background is a band of high and intermediate attenuation extending from the stations KASH and TGMT as far as CHM and TKM2. In the south the band extends along the Talas-Fergana fault, and turns north-northeast about KAZ. Figure 7 shows regression lines of *S*/*P* for the entire central Tien Shan, as well as for the line of high attenuation in the northern part of that band (between DGE, KAZ and CHM, TKM2). The regression line is seen to have a much greater slope for the high attenuation line. A very rapid decay in *S*/*P* is observed between the stations UCH, KZA and CHM, TKM2.

Comparatively high attenuation was recorded in the area of the Zaili Alatau Range (the station TLG), as well as in the southern margin of the Issyk-Kul' basin (the stations ULHL, KDS, and KAR). The greatest con-

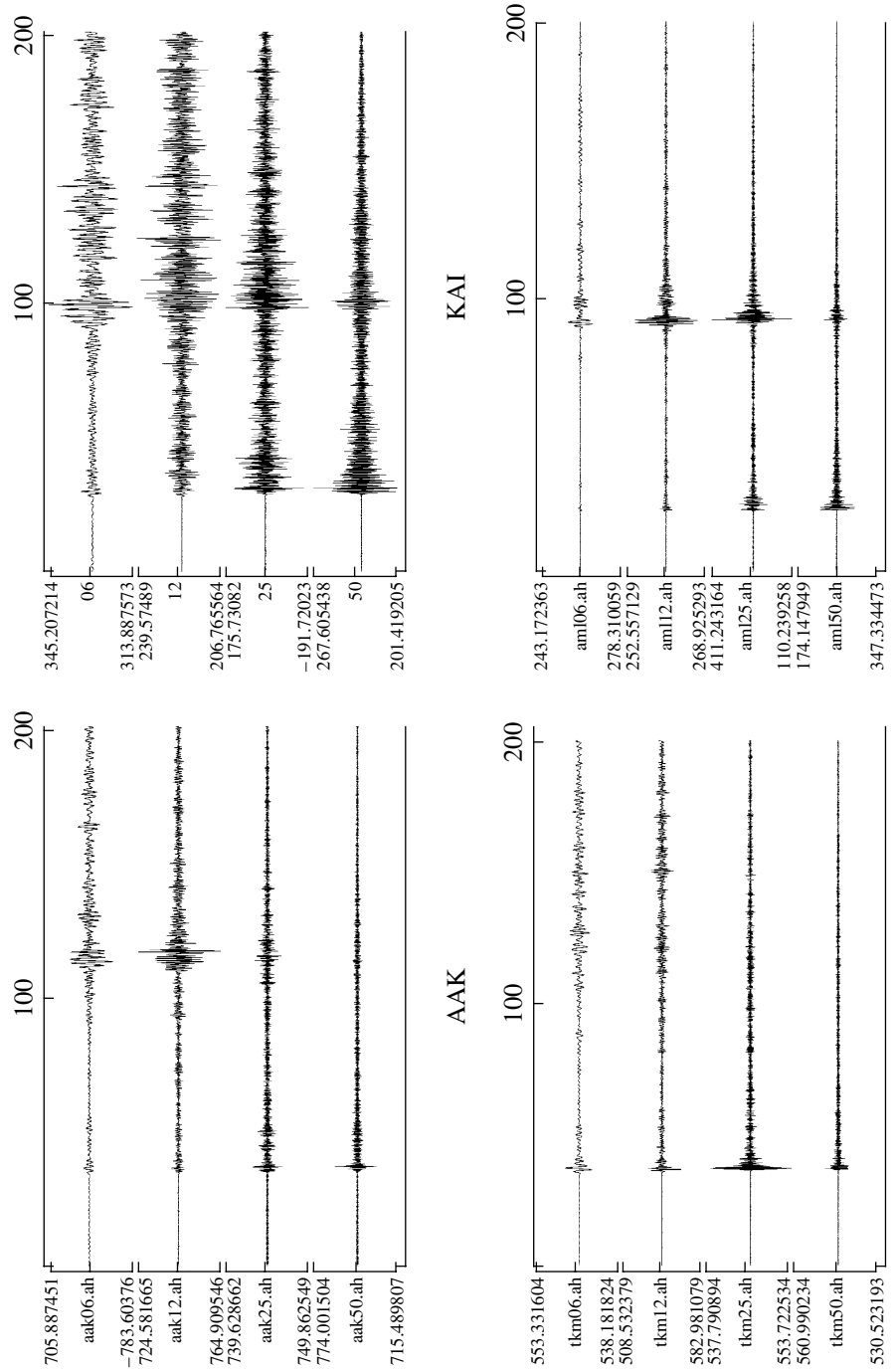

Fig. 6. Records of the October 10, 1999 earthquake made at several stations (vertical component). Channels (downward): 0.6, 1.25, 2.5, and 5 Hz. Time scale (in s) is at top.

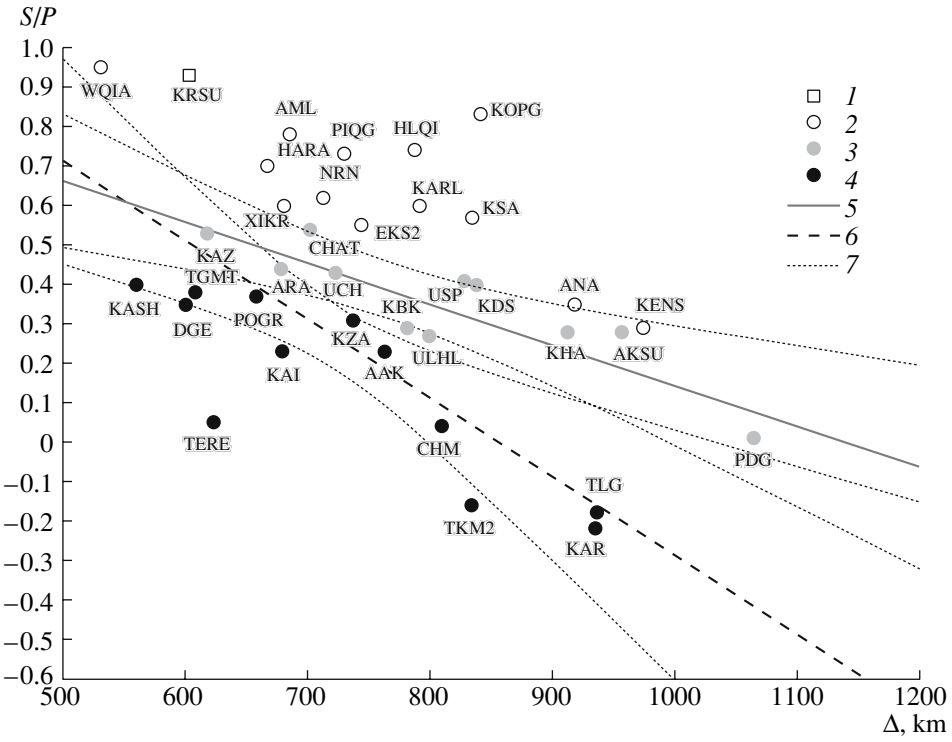

Fig. 7. The parameter *S*/*P* as a function of epicentral distance for the depth range 70–110 km. (*1*, *3*, *4*) 1998–2000 data, (*2*) 1991–1992 data. (*1–4*) attenuation: (*1*, *2*) low, (*3*) intermediate, (*4*) high. (*5*, *6*) regression lines: (*5*) for entire area, (*6*) for the north part of the high attenuation band, (*7*) confidence intervals for regression lines at 0.9 level.

trast between *S*/*P* over short distances occurs between ANA and KAR (0.57), WQIA and KASH (0.55), as well as between AML and ARA (0.34) and between EKS2 and AAK (0.32).

Consider the change in *S*/*P* for pairs of near stations approximately along the same ray and spaced within 100 km. For such pairs the *S*/*P* contrast is generally within 0.40. Upon this background the pairs AML–AAK ($\Delta S/P = -0.55$), KZA–TKM2 (–0.47), and especially WQIA–TERE (–0.90) stand out.

Figure 9 shows average values of *S*/c400 as a function of epicentral distance. It should be noted that the standard error of the mean values of that parameter for the stations considered here is much (about twice) lower than for *S*/*P*. The data scatter for different stations was also much lower than for the amplitude ratio of *S* and *P* waves. In contrast to this background, the station AML situated in the Suusamyr earthquake rupture zone has very high values of *S*/c400. Comparatively high values of *S*/c400 were also observed for the stations KRSU (the 1992 data), EKS2 and AAK installed within 60–70 km of the rupture zone.

At the same time comparatively low values of that parameter were obtained for most stations installed on young sedimentary rocks (in the northern margin of the Tarim massif, as well as for the station ARA).

Hypocentral depths 190–230 km. More data have been used for this depth range, primarily coming from the analog stations. We define a parameter $S/P_{100/200}$, which is the difference between the values of *S*/*P* for the depths 70–110 and 190–230 km. It turned out that $S/P_{100/200} = 0.07 \pm 0.23$ (an average based on 37 stations), that is, the *S*/*P* ratios for the two depth ranges are rather similar.

Figure 10 shows the average *S*/*P* plotted against epicentral distance. It is seen that the leading features in the distribution of that parameter persist for this depth range also. The differences in *S*/*P* for near epicentral distances exceed 1.0 log units. The comparatively low attenuation for the stations in the northwestern margin of the Tarim massif appears here too, as well as for the stations USP and ANA (Fig. 11). As well as the NRN station, comparatively low attenuation is also observed for the KAI station, which too is situated in the northern margin of the Naryn basin. Comparatively low attenuation is characteristic for KRSU and NICH, and especially TORK (the ray paths for these stations traverse the uppermost mantle beneath the eastern margin of the Fergana basin). Higher values of *S*/*P* were recorded at KUU (the Ili basin). For this depth range we have succeeded in identifying a band of high attenuation along the Zaili and Kungei Alatau ranges, between the stations TKM2 and SATY. Comparatively low attenuation is observed south of the Suusamyr rupture zone (AML).

When data at the same stations are compared, one notices how the southern part of the high attenuation

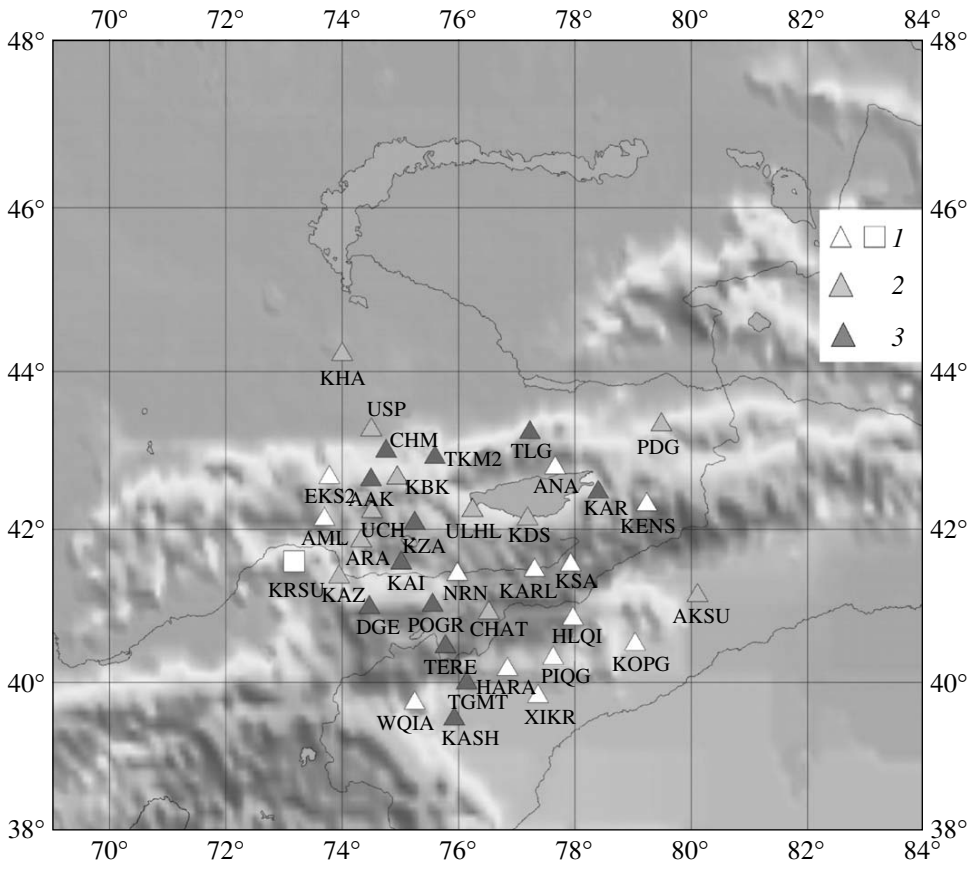

Fig. 8. Map showing variations in *S*/*P* for the depth range 70–110 km. Triangles denote the 1999–2000 data, the square is for 1991–1992. Station shading is analogous to that in Fig. 7. (*1*–*3*) Attenuation: (*1*) low, (*2*) intermediate, (*3*) high.

band moves toward the southwest with greater focal depth (increasing attenuation in the area of KAZ and WQIA is accompanied by decreased attenuation in the region between KAI and TGMT). At the same time, the comparatively high attenuation in the northern part of that band is retained. We note that the regression line for the northern part of the high attenuation band (between the stations DGE, KAZ and CHM, MTB) has a much higher slope than the overall value for the entire central Tien Shan, similar to that of the 70–110 km depth range (Fig. 10). The greatest contrast in *S*/*P* at short distances was recorded here between TGMT and KASH (0.61), KENS and KAR (0.50), AAK and KBK (0.48), and between KST and TKM2 (0.36).

For a pair of near stations on the same ray spaced closer than 100 km, the contrast in *S*/*P* is commonly below 0.45. At the same time, rather high values of $\Delta S/P$ are observed for the pair NRN–ULHL (–0.50), and especially for KZA–TKM2 (–0.70). It can thus be stated that *S*/P sharply decreased between KZA and TKM2 for both depth ranges.

Figure 12 shows the average *S*/c400 as a function of Δ. One again notices high values of *S*/c400 for the stations situated in the Suusamyr earthquake rupture zone or near it (the additional stations in this case were TORK and NICH which were also operated in 1991–1992). In addition, the *S*/c400 based on AML data was significantly (by 0.23 log units) higher in 1992 compared with 1999–2000. Relatively lower values of *S*/c400 were observed at most of the stations situated in the northwestern margin of the Tarim massif, as well as at ARA and NRN, in a manner similar to those found at shallower depths.

Figure 13 shows the overall *S*-coda envelopes for several stations installed in the Suusamyr earthquake rupture zone and near it constructed from the time of the *S*-wave peak amplitude. The envelope shapes differ significantly at times $t < 400$ s, exhibiting sharp inflections involving decreased and increased slope. Numerical modeling was used to show [7] that these inflections are due to the presence of zones of great attenuation contrast in the crust and uppermost mantle (in the case under consideration this refers to the close vicinities of the recording stations).

Envelopes at two stations are shown for different time intervals. It is seen that the coda decay rate for the TORK station, situated about 20 km from the Suusamyr rupture zone, experienced a dramatic increase in 1992 compared with 1980, while the rate for the KRSU station situated about 35 km further southward (away from

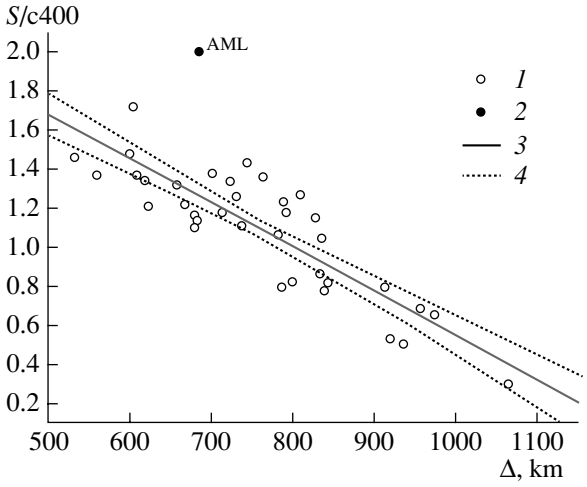

Fig. 9. The parameter *S*/c400 as a function of epicentral distance for the depth range 70–110 km. (*1*, *2*) Individual values (*2* denotes the station in the Suusamyr earthquake rupture zone), (*3*) regression line, (*4*) confidence intervals for regression lines at 0.9 level.

the rupture zone) significantly decreased in 1991–1992 compared with 1976–1977.

Comparison of *S*/*P* and *S*/c400 for the two depth ranges. We begin by examining in a little more detail how the values of *S*/*P* differ between stations for the two depth ranges studied here. Analysis shows that $S/P_{100/200}$ varies by nearly an order of magnitude, between 0.47 at KRSU and –0.49 at TERE. Figure 14 presents information on the stations that show significant differences in *S*/*P* between the two depth ranges: $|S/P_{100/200}| \geq 0.20$. It appears from this map that large values of the parameter were recorded for about one third of the stations used. Large positive values of the parameter ("pluses"), which indicate a rapid increase in attenuation with increasing depth in the uppermost mantle, are in the first instance observed at the stations situated in the margin of the Tarim massif (KASH with 0.46, WQIA with 0.45, and AKSU with 0.29), as well as in the northern part of the band of low *S*/*P* (KAZ with 0.24, UCH with 0.29, KBK with 0.33, and TKM2 with 0.30). Large "pluses" were also recorded at KARL (0.35), AML (0.33), and ANA (0.30).

Large "minuses" are found only at four stations which are situated northeast of the Talas–Fergana fault (POGR (–0.20) and TERE), as well as KHA (–0.31) and AAK (–0.21). It is of interest to note that these stations are aligned along a north-northwest trending line.

We note that the overwhelming majority of stations with high values of $|S/P_{100/200}|$ cluster in the west of the study area, the greatest station density being located around the Susamyr earthquake rupture zone.

The greatest contrast in $S/P_{100/200}$ for neighbouring stations was observed between WQIA and TERE

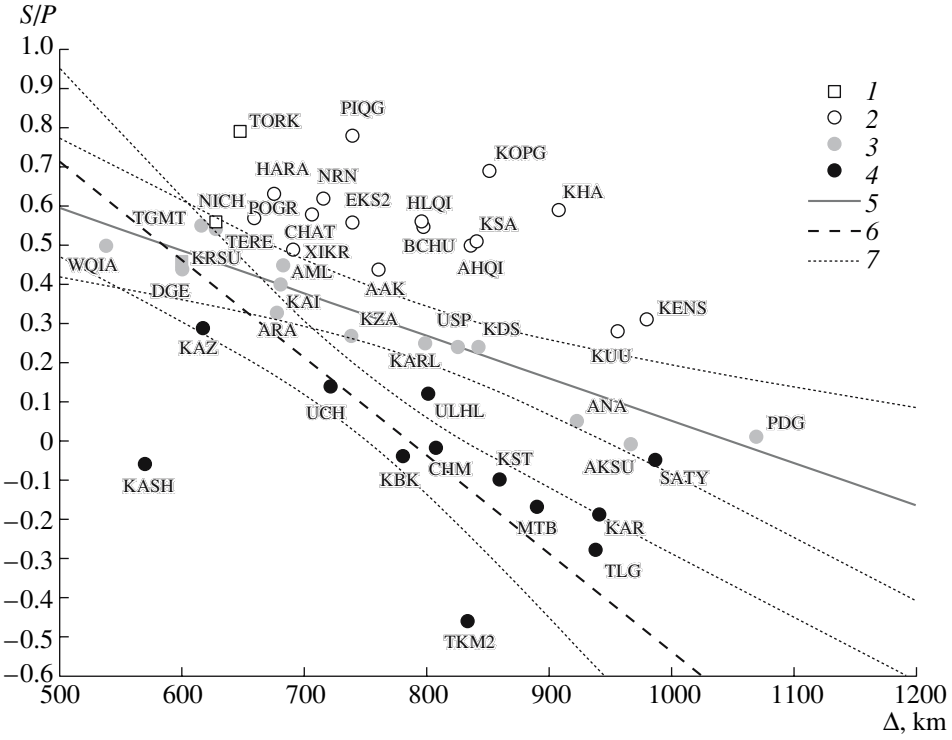

Fig. 10. The parameter *S*/*P* as a function of epicentral distance for the depth range 190–230 km. Attenuation: (*1*, *2*) low, (*3*) intermediate, (*4*) high. Regression lines: (*5*) for entire area, (*6*) for the north part of the high attenuation band, (*7*) confidence intervals for regression lines at 0.90 level.

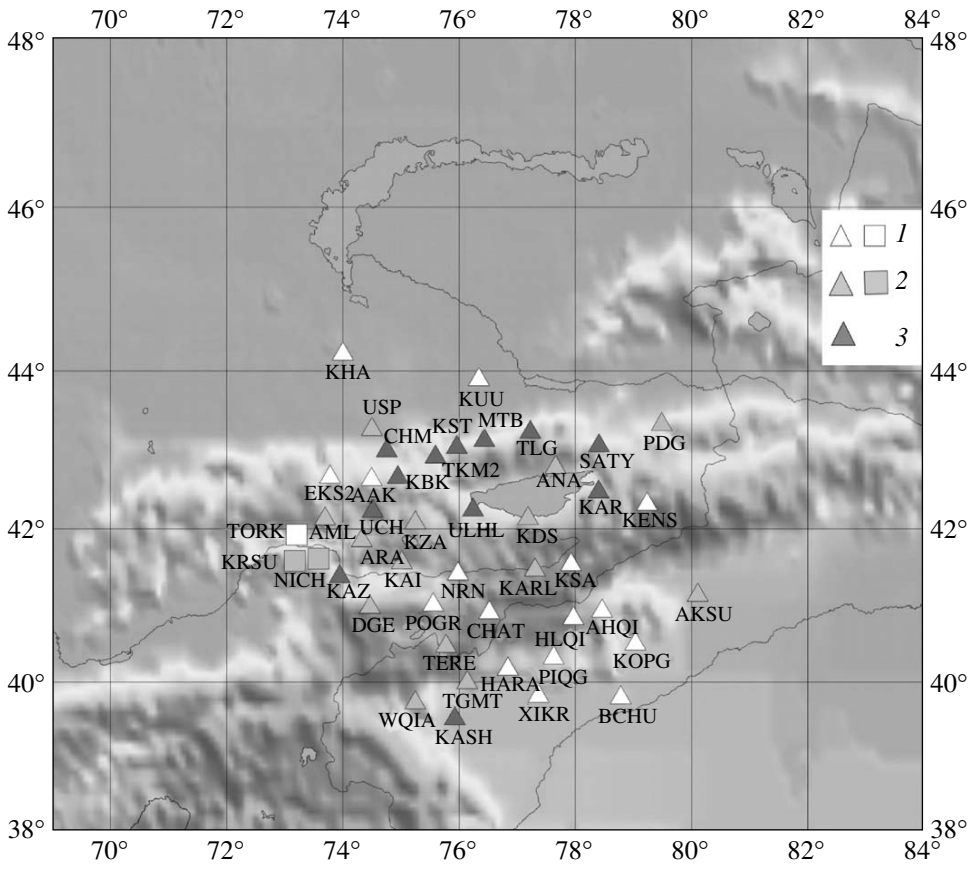

Fig. 11. Map showing variations in *S*/*P* for the depth range 190–230 km. The legend is as in Fig. 8.

(0.94); at shorter distances the greatest contrasts were between KASH and TGMT (0.63) and between AAK and KBK (–0.54).

Proceeding by analogy, we define the parameter $S/c400_{100/200}$, which is the logarithm of the ratio of *S*/c400 for the depths 70–110 and 190–230 km. The parameter is subject to much less scatter than is the case for $S/P_{100/200}$, and is smaller, exceeding 0.20 in absolute value at three stations only: TERE (–0.46), KSA (0.23), and XKER (–0.27). We note that the differences in both of these parameters, *S*/*P* and *S*/c400, were abnormally large at TERE for the two depth ranges.

Estimation of the upper mantle *Q*. We shall estimate the effective Q_s in the uppermost mantle from the variation of *S*/c400 with distance (Figs. 9, 12). We shall eliminate the obviously anomalous values of that parameter observed at AML and at near stations, all denoted by filled symbols in Figs. 9 and 12. To a first approximation the falloff of *S*-wave amplitude with hypocentral distance *r* can be described by the relation

$$A_s \sim \exp(-\pi r/Q_s c_s T)/r, \qquad (1)$$

where c_s is the average shear wave velocity in the upper mantle and *T* the period of wave motion. We then use the average relations of *S*/c400 versus distance to find for $c_s = 4.6$ km/s and $T = 0.8$ s:

$Q_s = 210 \pm 30$ and 210 ± 25, respectively, for hypocenters at depths of ~100 and 200 km.

Knowing Q_s, we can use the falloff of *S*/*P* with distance to estimate the average Q_p. From

$$A_s/A_p = \exp[-\pi r(1/Q_s c_s - 1/Q_p c_p)/T] \qquad (2)$$

with $c_p = 8.0$ km/s [33], we obtained $Q_p = 310 \pm 100$ and 370 ± 150, respectively, for hypocenters at depths of ~100 and 200 km.

Taking the above results into account and assuming the parameter Q_p/Q_s to be constant for each depth range, we can estimate Q_s and Q_p for the high attenuation band from Figs. 7 and 10 to find $Q_s \sim 125 \pm 30$ and 90 ± 15; $Q_p \sim 190 \pm 50$ and 160 ± 25, for hypocentral depths of 100 and 200 km, respectively.

Recalling the range of epicentral distance available in this study, we may conclude that the resulting *Q* estimates for hypocenters of $h_0 \sim 100$ km are relevant to the uppermost mantle (50–75 km depth) and to the depths 50–100 km in the case $h_0 \sim 200$ km.

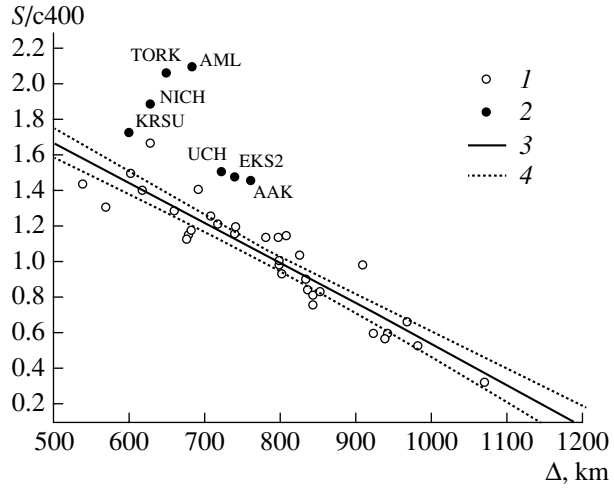

Fig. 12. The parameter *S*/c400 as a function of epicentral distance for the depth range 190–230 km. (*2*) Stations in the Susamyr earthquake rupture zone and close to it. The other notation is analogous to that in Fig. 9.

DISCUSSION

It was remarked above that the main differences in *S*/*P* accumulate in the crust and uppermost mantle, within about 130 km southwest of the relevant station. The available geophysical evidence helps refine that estimate. For example, it was shown in [4] that very low *S* velocities have been recorded down to 15 km depth in the eastern part of the Kirgiz Range, which must correspond with a very high attenuation. At the same time, we have data to show that rather large differences in *S*/*P* exist for three stations in the area (EKS2, AAK, and KBK), as large as 0.6 for hypocentral depths of ~200 km. From this we can infer that attenuation variations in the upper crust do not significantly affect the variation of *S*/*P*. In addition, judging from coda records of local earthquakes and quarry blasts, *S* waves have a general pattern of low attenuation in the middle crust and very high attenuation in the lower crust, at depths greater than 30 km [9, 14, 20]. This is consistent with MTS findings, according to which the lower crust in Tien Shan (in contrast to the middle crust) generally exhibits very high conductivity, which is thought to be due to the presence of brine fluid [24]. Lastly, it was shown [14, 20] that the Tien Shan lithosphere involves narrow zones of very high attenuation at depths of ~30–100 km. In view of this evidence, as well as considering the size of the Fresnel zone for the paths considered, we may conclude that the high *S*-wave attenuation in the records of Hindu Kush earthquakes is largely relevant to the lower crust and uppermost mantle (depths of ~30–100 km) at distances of ~30–130 km southwest of the stations concerned.

Spatial variations in the attenuation field structure. First, we observe that, since the average *S*/*P* values for the two depth ranges are similar, this allows us to disregard, in a first approximation, the dependence of

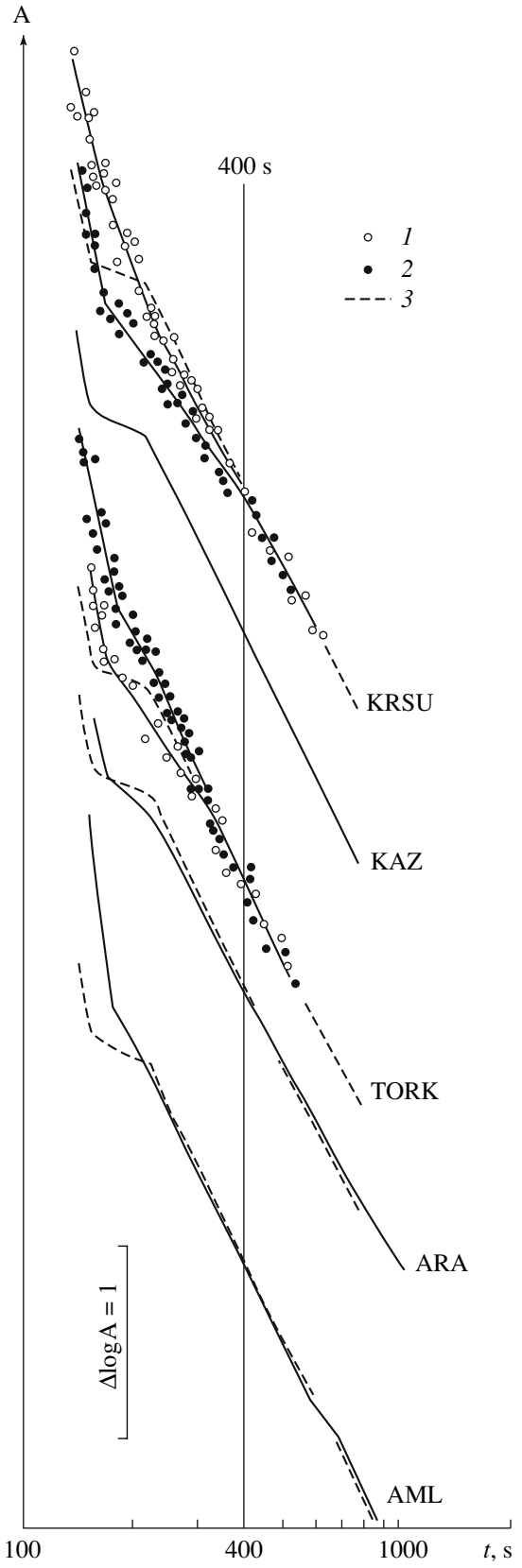

Fig. 13. *S*–coda envelopes for the stations installed in the Suusamyr earthquake rupture zone and close to it (depth range is 190–230 km). (*1*) 1976–1980 data, (*2*) 1991–1992 data, (*3*) envelope for the station KAZ.

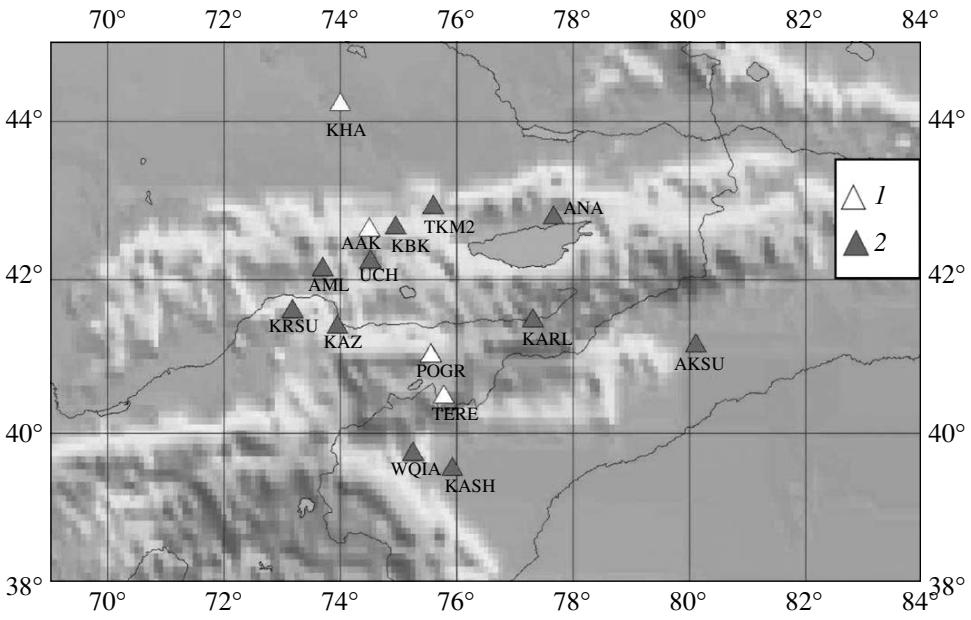

Fig. 14. Map showing variations in $S/P_{100/200}$ for the area of study. (*1*) Large negative values of the parameter, (*2*) large positive values.

effective upper mantle Q on depth for the paths between the Hindu Kush zone and Tien Shan. The comparatively high values of S/P at distances of ~500–600 km provide evidence of a relatively low attenuation of S waves in the upper mantle beneath the Pamirs, which was previously pointed out in [29].

It was shown in [9, 11, 14] that the Tien Shan lithosphere involves narrow zones of very low Q_s (40–50) upon the background of a generally high Q (the maximum values reach 1000–2000). Our estimates of effective Q_s are in general agreement with the previous results.

The new evidence also indicates a very strong spatial heterogeneity in the attenuation field in the lithosphere of the area of study. We note first of all that the results for S/P for both depth ranges indicate a generally low attenuation beneath major basins (the Chu, Ili, Issyk–Kul', Fergana, and Tarim basins). (Importantly, when mapping the parameter S/P, we did not even correct for high attenuation in the thick layer of young sedimentary rocks in the margin of the Tarim massif.) Lower attenuation was also recorded beneath the southern margin of the Kazakh Platform (the stations KHA and KUU).

At the same time, relatively low S-wave attenuation also occurs in some mountain regions, primarily, the Ketmen' (PDG) and Kokshaal ranges, as well as in the western Kirgiz Range. The band of high attenuation was also identified in the Zaili and Kungei Alatau ranges (which is consistent with the evidence supplied by the coda of local earthquakes and quarry blasts [14]), as well as beneath the Terskei Alatau Range and the eastern Kirgiz Range.

The most interesting feature of the field mapped here consists in a band of relatively high attenuation between the stations KASH and TKM2, which traverses several tectonic structures. One notes very low Q_s in the north of that band where the values are comparable with the estimates of Q for the northern Tibetan crust where evidence for Quaternary and recent volcanism is available, with these estimates being based on the falloff of Lg waves [26]. It should be stressed that the two largest earthquakes that have been recorded in Tien Shan during the past 25 years occurred at the boundaries of that band; these are the August 23, 1985 M = 7.0 Kashgar and the August 19, 1992 M = 7.3 Suusamyr events (Fig. 1). As well, the January 9, 1997 M = 5.9 earthquake also occurred there, in an area where no M ≥ 5.0 earthquakes had been known either in the historical record or instrumentally (around the DGE station).

The evidence on S/P for different depths of focus in the north of the band is consistent, thus favouring high attenuation down to comparatively great depths in the uppermost mantle, between the stations KZA and TKM2 primarily. The data we have relating to the coda envelopes of local earthquakes for the stations KBK, TKM2, UCH, and KZA, all strongly suggest high attenuation in the lower crust and uppermost mantle, in the depth range 30–90 km [20]. The attenuation rapidly decreases with increasing depth, which agrees with the very high values of S/P for the station KUU compared with KBK and TKM2 (Fig. 10).

The large difference in S/P for the southern part of the band allows a comparison to be made between the attenuation in the Talas–Fergana fault area and south-

west of it. Considering the degree to which the rays are offset in the uppermost mantle, it can be inferred from the data recorded at TGMT, TERE, POGR, and KAI that a thin layer of high attenuation exists just under the crust in the southeastern part of the fault zone. This makes the *S*-wave attenuation higher for hypocentral depths of ~100 km and lower for deeper hypocenters. An especially high attenuation in the uppermost mantle is observed between the stations WQIA and TERE. The overall crustal attenuation is comparatively low there, because otherwise the values of *S*/*P* for TERE could not have been above the average for hypocentral depths of about 200 km.

At the same time, southwest of the fault the layer of high attenuation plunges deeper, judging from the relatively high *S*/*P* values for hypocenters of ~100 km depth (WQIA and KAZ). One exception is DGE, the layer of high attenuation southwest of which is comparatively thick, as shown by relatively low *S*/*P* for both depth ranges.

It should be noted that the layer of high attenuation is nonexistent just under the M interface in the central part of the Talas–Fergana fault, judging by relatively low attenuation of *S* waves as recorded at AML and ARA from events of ~100 km depth.

Large positive values of $S/P_{100/200}$ suggest increasing *S*-wave attenuation with increasing depth below the M interface. As follows from Fig. 14, this effect is primarily observed for the high attenuation band referred to above, which provides evidence of the rather deep roots of that anomaly.

It follows from Figs. 9 and 12 that very high values of *S*/c400 are only observed for the Susamyr earthquake zone and environs (the stations AML, TORK, NICH, KRSU, UCH, EKS2, and AAK). The single exception is the TERE data (for the depth range 190–230 km).

From this we infer a major upper-mantle high attenuation anomaly related to the Suusamyr earthquake rupture zone. The anomaly size can be estimated from the coda of local earthquakes. Kopnichev and Sokolova [18] showed that a layer of high attenuation was identified at depths of 90–150 km around the station AML in 1999. At the same time, a narrow (no wider than 10 km) layer of very high attenuation existed around the TORK station in 1989–1990 whose thickness was much greater (depths of 45–180 km). We note that narrow subvertical low–*Q* zones in the lower crust and upper mantle were also found to exist beneath the rupture zone of the April 29, 1991 Racha, Georgia, North Caucasus earthquake [1].

The presence of the long subvertical layer of high attenuation can explain the anomalies in *S*/c400 around the TORK and AML stations. It was earlier remarked [15] that such a layer is a kind of waveguide which partially entraps (because its boundaries are imperfect) short period shear waves and partially serves as a screen for these waves. The coda model adopted here involves waves that are incident at increasingly higher angles on the M interface as time goes on, hence the screening effect of a vertical waveguide becomes progressively better defined for such waves. At the same time, the effective attenuation of *S* waves in the waveguide rapidly decreases at stations farther away from the rupture zone (EKS2, AAK).

It is of interest to compare attenuation and seismic velocities. We note that the low attenuation in the uppermost mantle beneath the Fergana basin is consistent with the firmly established fact of significant *S*-wave velocity increase at depths of 35–75 km in the area [33]. Unfortunately, it is impossible thus far to perform a similar comparison for the depth range 30–100 km in other areas of Tien Shan [34]. At the same time, the low attenuation in the uppermost mantle beneath the western Tarim and the southern margin of the Kazakh Platform is not inconsistent with the high velocities of P_n and *P* waves derived by tomography [25, 32]. Lastly, the characteristics of the attenuation field for the lower crust and uppermost mantle in central Tien Shan are in good agreement with the main parameters of *P*-wave velocity field (T.M. Sabitova, personal communication). Below we also compare the leading features in the shear wave attenuation fields derived by several different methods.

Time–dependent variations in the attenuation field structure. It follows from Fig. 13 and the *S*/c400 data for AML recorded in 1992 and 1999–2000 that the attenuation field structure in the Suusamyr earthquake rupture zone was experiencing substantial changes over time, both before the event and after it. This agrees with results from the coda of local earthquakes [19].

We wish to note that the *S*-wave attenuation field in the Tien Shan lithosphere was previously mapped in detail based on records of numerous local earthquakes as recorded in the 1970s by the supersensitive ZRN station installed in the Kokchetav massif, northern Kazakhstan. The method used was based on a comparison of amplitudes in Lg and the coda [11]. We are going to compare the mappings carried out in the 1970s and in the late 1990s taking into account certain differences in the methods (we mean the greater detail and the substantially lower accuracy obtainable from the parameter Lg/coda [11]).

First of all, we wish to emphasize similarities in the data obtained for the major basins, that is, the Tarim, Fergana, Chu, Ili, and Issyk Kul' basins, with low *S*-wave attenuation for both of these cases. In both there is also the band of high attenuation in the Zaili Alatau Range area, between the TKM2 and TLG stations.

At the same time, there are also considerable differences in the attenuation field structure. In the 1970s there was a narrow zone of high attenuation at the boundary between the Tarim and southern Tien Shan (probably it was not detected in the late 1990s merely because the mapping method based on the parameter *S*/*P* provides less detail). However, a well-defined band

of high attenuation was clearly discernible between the KASH and TKM2 stations in the late 1990s, which was absent 20–25 years earlier.

This relatively rapid change in the *S*-wave attenuation field structure can only have been due to a rearrangement of the fluid field in the crust and upper mantle. Judging by previous seismic evidence [1, 9,11], as well as MTS measurements [3], interrelated fluid–saturated channels which traverse various tectonic features in Tien Shan exist in the lower crust. The fluids can also rise to the crust from the upper mantle along the "roots" of major fault zones [16, 19, 30]. We remark in this connection that very high (submantle) helium isotope ratios were recorded in groundwater within the high attenuation band (in the Talas–Fergana fault zone) in the late 1980s (Fig. 1), such values had never before occurred outside areas of recent volcanism [22].

The rapid change in the attenuation field structure around KRSU and TORK during 12–15 years shows that the fluids were moving toward the Susamyr earthquake rupture zone prior to the event. As well, the attenuation anomaly in the AML area provides evidence of the preservation of channels for the rise of fluids 7–8 years after the Susamyr earthquake. This is consistent with the evidence of [19] as to the rise of mantle fluids in the rupture zones of large earthquakes during a few tens of years after the events. (We note that the low attenuation for hypocenters of ~100 km depth based on the WQIA data may also have been related to the rise of fluids from the uppermost mantle in the 1985 Kashgar earthquake rupture zone and environs some 13–15 years after that event [19]).

There is a great amount of geophysical [1, 3, 12, 13, 17, 19] and geochemical [2, 28, 30] evidence to demonstrate the importance of mantle fluids in the precursory processes of large earthquakes. In this connection the low seismicity of the basins with their lower attenuation in the lithosphere can be explained by a deficit of free fluids in the uppermost mantle [19]. We note that this conclusion is not at variance with the MTS data which yield very low conductivities for the lithosphere of the Naryn basin down to 90 km depth [24].

The very well pronounced anomaly in the attenuation field prior to the Suusamyr earthquake argues in favor of the methods proposed for detecting precursory changes in Tien Shan. The fact that the two largest (for the last 25 years) Tien Shan earthquakes occurred in the band of high attenuation suggests that the next large earthquake may also occur in the area of that anomaly. Of special interest in this connection is the north termination of the band (between KZA and TKM2) where a very high shear wave attenuation is observed along with a large contrast in S/P and $S/P_{100/200}$. We note in this connection that researchers at the Institute of Seismology of the Ministry of Education and Science in the Republic of Kazakhstan (to be referred to hereafter as IS MES RK) identified an extensive seismic quiescence south of TKM2 prior to 2004. The important fact is that earthquakes at depths of ~20 km depth have been recorded there since 1996 (an increase in the relative rate of comparatively deep events is known to be an important precursor [13]). We note that several comparatively large (M = 4.0–5.0), deep (h_0 ~ 20 km) earthquakes occurred in the area in 2004–2005 which can probably be regarded as foreshocks of a much larger event. Further, M.D. Imanbaeva et al. [6] report a geochemical anomaly in the KBK area for as long as four years consisting of a considerable decrease in the intensity of helium flux, with the flux at all the other stations in northern Tien Shan constantly increasing. T.P. Suslova (personal communication) noted a considerable increase in the content of carbon dioxide in groundwater at the IS MES RK geochemical stations closest to the anomalous region since early January 2004. The large attenuation anomaly in the area identified here, as well as the geophysical and geochemical evidence referred to above, all point to the necessity of special multidisciplinary studies to be conducted there with a view to intermediate–term and short–term prediction.

CONCLUSIONS

(1) Characteristics of the attenuation field of short period seismic waves in the lithosphere of central Tien Shan were derived from records of deep–focus Hindu Kush earthquakes.

(2) It has been found that the attenuation field in the area of study is highly heterogeneous. Relatively low attenuation is typical of major basins: the Chu, Ili, Issyk Kul', Naryn, Fergana, and Tarim basins. In the west of the study area is a band of high attenuation containing the rupture zones of the two largest earthquakes to have occurred in Tien Shan for the last 25 years, viz., the August 23, 1985 Kashgar and the August 19, 1992 Suusamyr earthquakes.

(3) Abnormally high values of S/c400 were obtained for the stations installed in the Suusamyr earthquake rupture zone and environs. For two of these stations we found well-pronounced time-dependent variations in the coda envelope before the earthquake.

(4) Q_s and Q_p in the upper 50-km mantle layer have been estimated. Effective Q-values for the band of high attenuation are about twice as small as those for the entire central Tien Shan.

(5) It was found that the attenuation field structure in the area of study has changed significantly during the last 20–25 years, which can only be related to an active rearrangement of the fluid field in the crust and uppermost mantle. The analysis of a set of geophysical and geochemical data suggests a high probability for the next large earthquake to occur in the northern part of the high attenuation band.

ACKNOWLEDGMENTS

The authors thank the IRIS DMC for their digital data and G. Pavlis for his aid in data selection and preprocessing.

REFERENCES

1. Aptikaeva, O.I., Aref'ev, S.S., Kvetinskii, S.I., et al., Heterogeneities in the Lithosphere and Asthenosphere: the Rupture Zone of the 1991 Racha Earthquake, *Dokl. RAN*, 1995, vol. 344, no. 4, pp. 533–538.
2. Asada, T., Ed., *Earthquake Prediction Techniques: Their Application in Japan*, University of Tokyo Press, 1982.
3. Berdichevskii, M.N., Borisova, V.P., Golubtsova, N.S., et al., An Interpretation of MT Soundings in the Minor Caucasus Mountains, *Fizika Zemli*, 1996, no. 4, pp. 99–117.
4. Vinnik, L.P., Kosarev, G.L., Oreshin, S.I., et al., The Tien Shan Lithosphere Derived from *P* and *S* Wave Receiver Function Data, in *Geodinamika i geoekologicheskie problemy vysokogornykh regionov* (The Geodynamics and Geoecologic Problems of High Mountain Regions), Moscow–Bishkek, 2003, pp. 94–105.
5. Zapol'skii, K.K., Frequency Selective Seismic Stations, in *Eksperimental'naya seismologiya* (Experimental Seismology), Moscow: Nauka, 1971, pp. 20–36.
6. Imanbaeva, M.D., Mozoleva, E.L., Yakovenko, V.S., et al., Variations in Hydrogeochemical Parameters Due to Geodynamic Processes, in *Geodinamika i geoekologicheskie problemy vysokogornykh regionov. Tezisy dokladov* (The Geodynamics and Geoecologic Problems of High Mountain Regions. Abstracts of Papers), Bishkek, 2002, p. 117.
7. Kaazik, P.B. and Kopnichev, Yu.F., Anomalous Envelopes of Lg Coda and their Interpretation Assuming an Earth Model with Laterally Varying Attenuation, *Vulkanol. Seismol.*, 1986, no. 5, pp. 64–74.
8. Kaazik, P.B., Kopnichev, Yu.F., Nersesov, I.L., and Rakhmatullin, M.Kh., An Analysis of Fine Structure in Short Period Seismic Waves Recorded by an Array, *Fizika Zemli*, 1990, no. 4, pp. 38–49.
9. Kvetinskii, S.I., Kopnichev, Yu.F., Mikhailova, N.N., et al., Lithosphere and Asthenosphere Heterogeneities in the Rupture Zones of Large Earthquakes in Northern Tien Shan, *Dokl. RAN,* 1993, vol. 329, no. 1, pp. 25–28.
10. Kopnichev, Yu.F., *Korotkoperiodnye seismicheskie volnovye polya* (Short Period Seismic Wave Fields), Moscow: Nauka, 1985.
11. Kopnichev, Yu.F. and Nurmagambetov, A.N., Detailed Mapping of Tien Shan Upper Mantle Using Attenuation of Shear Seismic Waves, *Fizika Zemli*, 1987, no. 10, pp. 11–25.
12. Kopnichev, Yu.F., Variations in the Attenuation Field of Shear Waves before Large earthquakes in Northern Tien Shan, *Dokl. RAN*, 1997, vol. 356, no. 4, pp. 528–532.
13. Kopnichev, Yu.F. and Mikhailova, N.N., Geodynamic Processes in the Rupture Zone of the November 12, 1990 Baisorun Earthquake, Northern Tien Shan, *Dokl. RAN*, 2000, vol. 373, no. 1, pp. 93–97.
14. Kopnichev, Yu.F., On the Fine Structure of the Crust and Upper Mantle at the Boundary of Northern Tien Shan, *Dokl. RAN,* 2000, vol. 375, no. 1, pp. 93–97.
15. Kopnichev, Yu.F., Long Period Time Variations in Attenuation Field in the Lithosphere and Asthenosphere of Northern Tien Shan, *Vulkanol. Seismol.*, 2001, no. 3, pp. 63–75.
16. Kopnichev, Yu.F. and Sokolova, I.N., Space–time Variations in the Structure of Shear Wave Attenuation Field: the Semipalatinsk Test Site, *Fizika Zemli*, 2001, no. 11, pp. 73–86.
17. Kopnichev, Yu.F., Baskutas, I., and Sokolova, I.N., Pairs of Large Earthquakes and Geodynamic Processes in Central and South Asia, *Vulkanol. Seismol.*, 2002, no. 5, pp. 49–58.
18. Kopnichev, Yu.F. and Sokolova, I.N., Variations in Shear Wave Attenuation Structure in the Rupture Zones of Large Earthquakes, in *2-i kazakhstansko-yaponskii seminar po prognozu zemletryasenii* (The Second Kazakhstan–Japan Seminar on Earthquake Prediction), Almaty, 2002.
19. Kopnichev, Yu.F. and Sokolova, I.N., Space–time Variations in *S*-wave Attenuation in the Rupture Zones of Large Tien Shan Earthquakes, *Fizika Zemli*, 2003, no. 5, pp. 73–86.
20. Kopnichev, Yu.F. and Sokolova, I.N., Heterogeneities in Shear Wave Attenuation in the Crust and Upper Mantle of Central Tien Shan, *Gornyi Zhurnal Kazakhstana*, 2004, no. 5, pp. 25–29.
21. Krestnikov, V.N., Belousov, T.P., Ermilin, V.I., et al., *Chetvertichnaya tektonika Pamira i Tyan'-Shanya* (Quaternary Tectonics of the Pamirs and Tien Shan), Moscow: Nauka, 1979.
22. Polyak, B.G., Kamenskii, I.L., Sultankhodzhaev, V.A., et al., Submantle Helium in the Fluids of Southeastern Tien Shan, *Dokl. AN SSSR*, 1990, vol. 312, no. 3, pp. 721–725.
23. Aptikaeva, O.I. and Kopnichev, Yu.F., Space–time Variations of the Coda Wave Envelopes of Local Earthquakes in the Region of Central Asia, *J. Earthq. Pred. Res.*, 1993, vol. 2, no. 4, pp. 497–514.
24. Bielinski, R., Park, S., Rybin, A., et al., Lithospheric Heterogeneity in the Kyrgyz Tien Shan Imaged by Magnetotelluric Studies, *Geophys. Res. Lett.*, 2003, vol. 30, no. 15, DOI: 10.1029/2003GL017455.
25. Chen, Y., Roecker, S., and Kosarev, G., Elevation of the 410 km Discontinuity Beneath the central Tien Shan: Evidence for a Detached Lithospheric Root, *Geophys. Res. Lett.*, 1997, vol. 24, pp. 1531–1534.
26. Fan, G. and Lay, T., Characteristics of Lg Attenuation in the Tibetan Plateau, *J. Geophys. Res.*, 2002, vol. 107, no. B1, doi: 10.1029/2001JB000804.
27. Hammond, W. and Humpreys, E., Upper Mantle Seismic Wave Velocity: Effects of Realistic Partial Melt Geometries, *J. Geophys. Res.*, 2000, vol. 105, pp. 10975–10986.
28. Italiano, F., Martinelli, G., and Nuccio, P., Anomalies of Mantle-derived Helium during the 1997–1998 Seismic Swarm of Umbria–Marche, Italy, *J. Geophys. Res.*, 2001, vol. 28, no. 5, pp. 839–842.
29. Khalturin, V.I., Rautian, T.G., and Molnar, P., The Spectral Content of Pamirs–Hindu Kush Intermediate Depth

Earthquakes: Evidence for High–*Q* Zone in the Upper Mantle, *J. Geophys. Res.*, 1977, vol. 82, no. 20, pp. 2931–2943.

30. Kopnichev, Yu.F. and Sokolova, I.N., Mantle Helium Near Source Zones of Strong Earthquakes, *Abstr. General Assembly IASPEI*, Santiago, Chile, 2–8 October 2005.
31. Krestnikov, V.N., Nersesov, I.L., and Stange, D.V., The Relationship between the Deep Structure and Quaternary Tectonics of the Pamirs and Tien Shan, *Tectonophysics*, 1984.
32. Liang, C. and Song, X., Tomographic Inversion of P_n Travel Times in China, *J. Geophys. Res.*, 2004, vol. 109, no. B11304, doi:10.1029/2003JB002789.
33. Roecker, S., Sabitova, T.M., Vinnik, L.P., et al., Three–dimensional Elastic Wave Velocity Structure of the Western and Central Tien Shan, *J. Geophys. Res.*, 1993, vol. 98, no. B9, pp. 15779–15795.
34. Vinnik, L.P., Reighber, C., Aleshin, I., et al., Receiver Function Tomography of the Central Tien Shan, *Earth Planet. Sci. Lett.*, 2004, vol. 225, pp. 131–146.